arXiv:1703.00435v2 [quant-ph] 3 Mar 2017

Quantum Noise in Soliton Matterwave Interferometry

Simon A. Haine

*Department of Physics and Astronomy, University of Sussex, Brighton BN1 9QH, United Kingdom**

There has been considerable recent interest in matterwave interferometry with bright solitons in quantum gases with attractive interactions, for applications such as rotation sensing. We model the quantum dynamics of these systems and find that the attractive interactions required for the presence of bright solitons causes quantum phase-diffusion, which severely impairs the sensitivity. We propose a scheme that partially restores the sensitivity, but find that in most cases it is still better to work in a regime with minimal interactions.

Introduction— Rotation sensors based on matterwave interferometers have the potential to provide state of the art sensing capabilities [1]. An important criteria for producing an interferometer that is sensitive to rotations is that the matterwaves must traverse a trajectory which includes two or more possible paths that enclose a spatial area, with larger areas usually leading to higher sensitivity [2]. The current pursuits towards fulfilling this potential can be divided into two main approaches: *Free-space* atom interferometers, which operate in free-fall and use optical transitions between momentum modes to achieve spatial path separation [3–8], or *guided* configurations which involves the propagation of atoms along some guiding potential to achieve spatial path separation, analogous to an optical fibre [9–15]. While both approaches have their benefits and draw-backs, one attraction towards guided configurations is the potential for a very large enclosed area [12]. However, guided matterwave interferometery often requires working in a regime where atom-atom interactions are important, leading to complications in the matterwave dynamics [11, 15, 16]. One approach to minimize the effect of this classical multimode dynamics is to work with atomic gases with attractive interaction in the soliton regime [17–25]. In fact, it has recently been shown that soliton interferometry can provide higher fringe contrast than non-interacting gases [25–27]. However, so far these investigations have ignored the effects of *quantum noise* on the sensitivity of an interferometer. It is well known from quantum optics that non-linear interactions couple number fluctuations into phase-fluctuations [28–30]. In this letter, we find that this mechanism severely degrades the sensitivity when compared to non-interacting gases. However, we find that for intermediate interaction strengths, a modification to the scheme to include the addition of a state-preparation step can partially recover the sensitivity, but argue that it is usually better to minimize the interactions if possible, rather than working in the soliton regime.

Model— Our scheme is described in Fig. (1). We model a system where two counter-propagating matterwave solitons traverse a toroidal trapping potential in opposite directions and are interfered, with the goal of estimating the magnitude of a rotational frequency Ω. We consider a Bose gas with attractive interactions consisting of two hyperfine components (electronic states $|+\rangle$ and $|-\rangle$), with bosonic annihilation operators $\hat{\psi}_+(\mathbf{r})$ and $\hat{\psi}_-(\mathbf{r})$ respectively, which obey they usual bosonic commutation relations: $\left[\hat{\psi}_i(\mathbf{r}), \hat{\psi}_j^\dagger(\mathbf{r}')\right] = \delta(\mathbf{r}-\mathbf{r}')\delta_{ij}$. An initial state is created consisting of a soliton that has been coherently split into the two hyperfine components, with the $|+\rangle(|-\rangle)$ component propagating (anti-)clockwise around the ring. Such a state could be created by beginning with a stationary single component soliton and using a 2-photon Raman transition to coherently split it into different hyperfine states while transferring momentum $\pm\hbar\mathbf{k}$ to each component [16, 31]. After time $T = 2\pi Rm/\hbar k$, the two components have each traversed the ring and we apply another Raman coupling pulse to act as an atomic *beamsplitter*, which performs the transformation $\hat{\psi}_\pm \to \frac{1}{\sqrt{2}}(\hat{\psi}_\pm - i\hat{\psi}_\mp e^{\pm 2i\mathbf{k}\cdot\mathbf{r}})$, before the population in each component is measured and used to infer the phase difference accrued, and therefore estimate Ω. As in [10, 11, 15, 25], working in cylindrical coordinates, $\{r, \theta, z\}$, we assume a trapping potential of the form $V(\mathbf{r}) = \frac{1}{2}m\left[\omega_z^2 z^2 + \omega_r^2(r-R)^2\right]$ where R is the radius of the torus and ω_z and ω_r are the axial and radial trapping frequencies. Assuming that the radial and axial confinement is sufficiently tight, we may ignore the

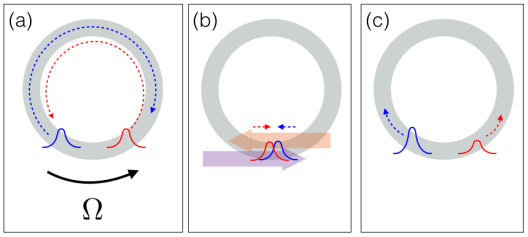

FIG. 1. (Color Online) (a): Matterwave solitons formed from a two-component BEC (blue: $|+\rangle$, red: $|-\rangle$) propagate around the ring in opposite directions, accumulating a phase-difference due to the external rotation frequency Ω. (b): After one complete circuit, the two components are interfered via a two-photon Raman transition, and the phase difference is converted into population difference (c).

dynamics in these directions. In terms of the coordinate $\xi = \theta R$, the effective Hamiltonian for the system is

$$\mathcal{H} = \sum_{j=+,-} \int \hat{\psi}_j^\dagger(\xi)\hat{H}_0\hat{\psi}_j(\xi)d\xi + \sum_{i,j=+,-} \frac{g_{ij}}{2}\int \hat{\psi}_j^\dagger(\xi)\hat{\psi}_i^\dagger(\xi)\hat{\psi}_j(\xi)\hat{\psi}_i(\xi)d\xi\,, \quad (1)$$

where $\hat{H}_0 = \frac{-\hbar^2}{2m}\frac{\partial^2}{\partial\xi^2} - \Omega\hat{L}_z$, and $\hat{L}_z$ is the z component of the angular momentum, and we have assumed that we are working in a frame rotating around the z-axis at angular frequency Ω. g_{ij} is the two-particle contact potential interaction strength between state $|i\rangle$ and $|i\rangle$ atoms. For convenience, we assume that $g_{++} = g_{--} \equiv g_0 \leq 0$, and $g_{+-} = 0$. The value of g_{+-} has very little effect on the results as for most of the duration the two components are not spatially overlapping [32].

To model the system we choose the initial state $|\Psi(0)\rangle = \mathcal{D}(\hat{a}_+,\alpha)\mathcal{D}(\hat{a}_-,\alpha)|0\rangle$, where $\mathcal{D}(\hat{a}_\pm,\alpha) = \exp(\alpha\hat{a}_\pm^\dagger - \alpha^*\hat{a}_\pm)$ is the Glauber coherent displacement operator, $\alpha = \sqrt{N_t/2}$, where N_t is the total mean number of atoms, $\hat{a}_\pm = \int\Psi_\pm^*\hat{\psi}_\pm d\xi$, and $\Psi_\pm(\xi) = A\,\mathrm{sech}(\sqrt{2m|\mu|/\hbar^2}\xi)e^{\pm ik\xi}$, where A is a normalisation constant such that $\int_{-\pi R}^{\pi R}|\Psi_\pm|^2 d\xi = 1$. The chemical potential μ is related to the total number N_t by $\mu = N_t^2 g_0^2 m/8\hbar^2$. It has previously been shown that the dynamics of such systems is reasonably insensitive to the *total* population statistics, but *is* sensitive to the statistics of the population *difference* [33]. We chose a two-mode Glauber coherent state for our initial state as it reflects the number difference statistics that are obtained from coherent splitting of ensembles of atoms. That is, there is no particle entanglement between the modes, as each atom is in a coherent superposition of states $|1\rangle$ and $|2\rangle$. Alternatively, we could have used a coherent spin state [34], which also has this property but for a well-defined total number of atoms. However a Glauber coherent state is much less computationally demanding for the numerical technique employed in this work.

We simulate the dynamics of the system by using a stochastic phase space technique known as the Truncated Wigner (TW) method, which has been described in detail elsewhere [35–37]. Briefly, the Heisenberg equations of motion can be converted into a Fokker-Planck equation (FPE) by using the correspondences between the quantum operators and Wigner function. By truncating third- and higher-order derivatives, the FPE is mapped onto a set of stochastic partial differential equations for the complex field for the jth component $\psi_j(\xi,t)$:

$$i\dot{\psi}_j = \left[\hat{H}_0 + g_0(|\psi_j|^2 - \frac{1}{\Delta})\right]\psi_j\,, \quad (2)$$

where Δ is the element that characterises the discretization of the spatial grid. After the solitons have each traversed one closed loop, the atomic beam-splitter is implemented via the transformation $\psi_\pm \to \frac{1}{\sqrt{2}}(\psi_\pm - i\psi_\mp e^{\pm 2ik\xi})$. By averaging over many trajectories with initial conditions sampled from the Wigner quasi-probability distribution, expectation values of quantities corresponding to symmetrically ordered operators in the full quantum theory can be obtained via the correspondence $\langle\{f(\hat{\psi}_j^\dagger,\hat{\psi}_j\}_{\mathrm{sym}}\rangle = \overline{f[\psi_j^*,\psi_j]}$, where 'sym' denotes symmetric ordering and the overline deonotes the mean over many stochastic trajectories. The initial conditions for the simulations are chosen as $\psi_\pm(\xi,0) = \sqrt{N_t/2}\Psi_\pm(\xi) + \eta_\pm(\xi)$, where $\eta_\pm(\xi)$ are complex Gaussian noises satisfying $\overline{\eta_m^*(\xi_i)\eta_m(\xi_j)} = \frac{1}{2}\delta_{n,m}\delta_{i,j}$. After solving equations [2] numerically on a spatial grid with 512 points, we calculate the expectation value and variance of the number of particles in each component after the final beam-splitter pulse. If we use the difference in population of each component $\hat{N}_d \equiv \int_{-\pi R}^{\pi R}(\hat{\psi}_+^\dagger\hat{\psi}_+ - \hat{\psi}_-^\dagger\hat{\psi}_-)d\xi$ as our signal, then the rotation sensitivity is given by

$$\Delta\Omega = \sqrt{\frac{V(\hat{N}_d)}{(\partial_\Omega\langle\hat{N}_d\rangle)^2}}\,. \quad (3)$$

We calculate $\partial_\Omega\langle\hat{N}_d\rangle$ by using finite difference and simulating small variations of Ω around $\Omega = 0$. Fig. (2) (red squares) shows the rotation sensitivity as a function of the interaction strength g_0. We see that as $|g_0|$ increases, the sensitivity is rapidly degraded. For comparison, we have also modelled a noninteracting gas, with a gaussian initial wave-packet with the same quantum statistics. The sensitivity in this case is very close to the naive standard quantum limit for rotation sensing (SQL): $\Delta\Omega_S = \frac{\hbar}{2mA}\frac{1}{\sqrt{N_t}}$ [15].

Two-mode model— We can understand this degradation in sensitivity by modelling the system with a simple 'two-mode' model [33, 38–40]. Specifically, we make the approximation $\hat{\psi}_\pm(\xi) \approx \hat{a}_\pm\Psi_+(\xi)$ in Eq. (1), which gives $\mathcal{H} = \mathcal{H}_0 + \mathcal{H}_{int}$, with

$$\mathcal{H}_0 = E_k\sum_{j=+-}\hat{a}_j^\dagger\hat{a}_j + \hbar\Omega Rk\left(\hat{a}_+^\dagger\hat{a}_+ - \hat{a}_-^\dagger\hat{a}_-\right)\,, \quad (4)$$

$$\mathcal{H}_{int} = \frac{\hbar\chi}{2}\left(\hat{a}_+^\dagger\hat{a}_+^\dagger\hat{a}_+\hat{a}_+ + \hat{a}_-^\dagger\hat{a}_-^\dagger\hat{a}_-\hat{a}_-\right)\,, \quad (5)$$

where $E_k = \frac{-\hbar^2}{2m}\int_{-\pi R}^{\pi R}\Psi_+^*\frac{\partial^2}{\partial\xi^2}\Psi_+ d\xi$ and $\chi = \frac{g_0}{2}\int_{-\pi R}^{\pi R}|\Psi_+|^2 d\xi \approx g_0^2 N_t m/4\hbar$. Moving to an interaction picture where the operators evolve under $\mathcal{H}_0$ and our state evolves under $\mathcal{H}_{\mathrm{int}}$, and expressing the state in the Fock basis gives

$$|\Psi(T)\rangle = e^{-2|\alpha|^2}\sum_{n_1=0}^{\infty}\sum_{n_2=0}^{\infty}\frac{\alpha^{n_1}}{\sqrt{n_1!}}\frac{\alpha^{n_2}}{\sqrt{n_2!}}|n_1,n_2\rangle e^{-i\Phi_{n_1,n_2}}\,, \quad (6)$$

where $\Phi_{n_1,n_2} = \frac{1}{2}\chi T\left[n_1(n_1-1) + n_2(n_2-1)\right]$. Introducing the psuedo-spin operators $\{\hat{J}_x = \frac{1}{2}(\hat{a}_+\hat{a}_-^\dagger +$

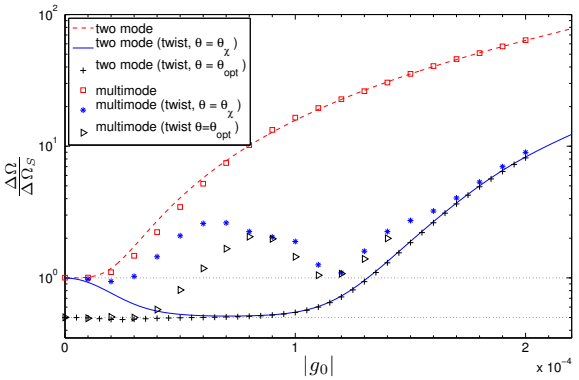

FIG. 2. (Color Online) Rotation sensitivity as a function of g_0 (g_0 is expressed in units of $2\pi\hbar/(mR^2)$). Red squares: Multi-mode TW model. Red dashed line: Analytic two-mode model. Blue solid line (Blue stars): Two-mode (multi-mode), TW model of pre-twisting scheme using $\theta = \theta_\chi$. Black triangles (plus symbols): Multi-mode (two-mode) TW model of pre-twisting scheme with a numerically optimised $\theta = \theta_{\rm opt}$ for each point. The upper black dotted line indicates $\Delta\Omega_S$, and the lower black dotted line indicates $\frac{1}{2}\Delta\Omega_S$, which is the standard sensitivity for matterwaves traversing two revolutions of the loop. Parameters: $N_t = 10^4$ and $k = 80/R$ for all simulations, which corresponds to a maximum interaction parameter of $\chi T = 7.6 \times 10^{-3}$.

$\hat{a}_+^\dagger\hat{a}_-)$, $\hat{J}_y = \frac{i}{2}(\hat{a}_+\hat{a}_-^\dagger - \hat{a}_+^\dagger\hat{a}_-)$, $\hat{J}_z = \frac{1}{2}(\hat{a}_+^\dagger\hat{a}_+ - \hat{a}_-^\dagger\hat{a}_-)\}$, the operators before ($t = T$) and after ($t = t_f$) the final beamsplitter are related by $\hat{J}_z(t_f) = -(\cos\phi_S\hat{J}_y(T) + \sin\phi_S\hat{J}_x(T))$ where $\phi_S = \Omega kRT$. At the most sensitive operating point ($\Omega = 0$), Eq. (3) becomes $\Delta\Omega = \frac{\hbar}{2mA}\sqrt{V(\hat{J}_y)/\langle\hat{J}_x\rangle^2}$. Using Eq. (6), we obtain

$$V(\hat{J}_y) = \frac{N_t}{4} + \frac{N_t^2}{8}\left(1 - \exp\left[-2N_t\sin^2(\chi T)\right]\right), \quad (7)$$

$$\langle\hat{J}_x\rangle = \frac{N_t}{2}\exp\left[N_t\left(-1 + \cos(\chi T)\right)\right]. \quad (8)$$

Fig. (2) (red dashed line) shows that our analytic model gives excellent agreement with our multi-mode numeric calculations.

Pre-twisting to reduce the effects of phase diffusion— We can partially restore the sensitivity by implementing a pre-twisitng scheme to undo the quantum noise added due to $\mathcal{H}_{\rm int}$. Fig. (3) shows a quasi-probability distribution formed from individual trajectories from a 2-mode TW simulation evolving under $\mathcal{H}_{\rm int}$. Initially, the individual trajectories are spread out in both J_z and J_y. However, after a period of evolution, the spread in J_z is coupled into a much larger spread in J_y, which is the origin of the degradation in sensitivity. By applying a rotation $\hat{U}_\theta = \exp(i\theta\hat{J}_x)$, the state is twisted such that another period of evolution under $\mathcal{H}_{\rm int}$ approximately restores the initial state. However, the nonlinear nature of $\mathcal{H}_{\rm int}$ means that this process breaks down for larger values of χT, as can be seen in the lower panels of fig. (3).

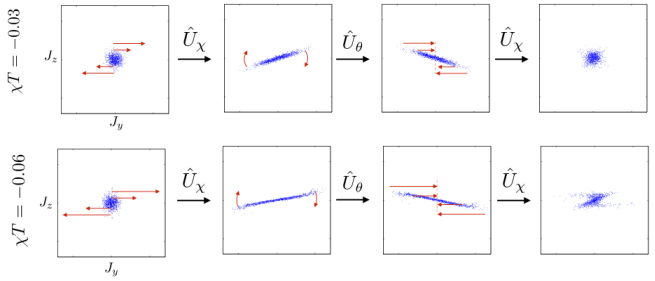

FIG. 3. (Color Online) Quasi-probability distribution for the pre-twisting sequence. Left to right: $|\Psi_0\rangle$, $\hat{U}_\chi|\Psi_0\rangle$, $\hat{U}_\theta\hat{U}_\chi|\Psi_0\rangle$, and $\hat{U}_\chi\hat{U}_\theta\hat{U}_\chi|\Psi_0\rangle$, for $\hat{U}_\chi = \exp(-i\mathcal{H}_\chi T/\hbar)$. Top line: $\chi T = -0.03$. Bottom line: $\chi T = -0.06$. For visual clarity, a reduced number of atoms ($N_t = 100$) was used.

We note that this could also have been achieved by reversing the sign of the χ. However, this is incompatible with the use of solitons as they require a negative interaction constant. The rotation angle $\theta = \theta_\chi$ that performs the rotation illustrated in fig. (3), is derived in the supplementary material [41].

The sensitivity that this scheme provides is represented by the blue line on fig. (2). There are two factors that influence the sensitivity. The first is the reduction in quantum noise ($V(J_y)$) due to this pre-twisting scheme. The second is that the θ rotation has a non-trivial effect on $d\langle S\rangle/d\phi$ due to the interplay between the phase shift accumulated before and after the rotation, with $\theta = 0$ leading to twice the slope as for a single period of evolution, and $\theta = \pi$ causing the two periods of phase accumulation to cancel. As such, for small values of χT, θ_χ is not the optimum angle, which is obtained via numerical optimisation, and the sensitivity that this yields is shown in fig. (2) (black crosses).

We implement the pre-twsiting scheme in our multi-mode model by replacing the final 50/50 beamsplitter of the single loop scheme with a variable angle beam splitter performing the transformation $\psi_\pm \to \psi_\pm\cos\theta - i\psi_\mp\sin\theta\exp(\pm 2ik\xi)$, and then allowing the solitons to perform a second circuit of the ring before finally being interfered with a 50/50 beamsplitter. Again, such a transformation is easily implemented via a coherent two-photon Raman transition. However, when assessing the performance of this scheme (fig. (2) blue stars), we see that while there is generally some improvement in sensitivity when compared to the original scheme, there is a significant discrepancy between the 2-mode model and the multi-mode model. In particular, the multi-mode model predicts significantly worse sensitivity than compared to the two-mode model. For larger values of g_0, the multi-mode model still gives about an order of magnitude improvement compared to the original scheme, but this is still worse than what would be obtained by using a non-interacting gas. In an attempt to further improve the sensitivity, we numerically optimised θ (fig. (2) black tri-

angles). This results in significant improvement for small values of g_0. However, the 'bump' for intermediate values of g_0 is still present. We speculate that the origin of this behaviour is due to the density gradients in the soliton coupling the quantum noise into other spatial modes such that the two-mode model no longer holds. The reason it is more noticible in the pre-twisting scheme is that the addition of $\hat{U}_\theta$ makes the final sensitivity far more sensitive to the quantum state, as a small over- or under-rotation can couple large amounts of phase noise into the J_z quadrature, which $\hat{U}_\chi$ then converts into additional phase-noise. As different regions of the soliton likely experience different degrees of phase-shearing, it is likely that this washes out the ability to adequately revive the quantum state. Finally, we also modelled a single component system where the beam-splitting was performed by quantum reflection/transmission from a narrow barrier as in [25]. For the single-loop scheme we found almost identical results to the two-component system. However, when trying to implement the pre-twisting scheme by varying the height of the barrier to implement $\hat{U}_\theta$, we found very little improvement than compared to the single-loop scheme. This was partly due to the difficulty in controlling θ and the phase of the outgoing matterwaves after interaction with the barrier.

Discussion— We found in [15] that the wave-packet dispersion of non-interacting matterwaves did not adversely effect the sensitivity. As such, our results generally indicate that the perceived benefits of solotonic matterwaves - the absence of wavepacket dispersion - are usually out-weighed by the loss of sensitivity due to the atomic interactions increasing the quantum noise. Previous theoretical studies [25–27] have observed an *increase* in the interferometric sensitivity due to the steepening of the interference fringe. However, these studies have all been based on mean-field models where the quantum noise has been neglected. We will now argue why this perceived increase in sensitivity may be an artefact of the mean-field model, and may not be present in full quantum many-body treatment of the system, or at least warrant a further investigation with a model that includes many-body effects. In Negretti *et al.* [26], a phase shift is imprinted on one portion of the BEC, before a period of evolution with the nonlinear interactions apparently 'amplifying' the observed dependency of the density on the phase shift. However, the metrological sensitivity is bounded by the Quantum Cramer-Rao Bound, which states that the minimum resolvable phase shift is given by $\Delta\phi \geq 1/\sqrt{F_Q}$, where F_Q is the Quantum Fisher Information [42]. By expressing the dynamics in terms of unitary operators such that the final quantum state of the system is $|\Psi_f\rangle = \hat{U}_{\rm int}\hat{U}_\phi|\Psi_0\rangle$, where $\hat{U}_{\rm int}$ is the unitary operator that describes the evolution after the phase imprinting, and $\hat{U}_\phi = \exp(-i\phi\hat{G})$ is the unitary operator for the phase imprinting step, for some Hermitian operator $\hat{G}$, its easy to show that $F_Q = 4V(\hat{G})$ where the variance is calculated with respect to the initial state $|\Psi_0\rangle$. As such, the Unitary operator $\hat{U}_{\rm int}$ does not contribute to the metrological sensitivity. The resolution to this apparent paradox is that the equation simulated by Negretti *et al.* (the Gross-Pitaevskii equation) *cannot* be described by a set of unitary operators acting on some initial state. However, the *full* quantum dynamics of the system *must* be described by unitary evolution, and hence the apparent increase in sensitivity may be an artefact of the simplified mean-field model rather than a feature of the true evolution of the system. Similarly, in Helm *et al.* [25], a steepening on the interference fringe was also observed. The nonlinear component of the Hamiltonian and the generator of rotation do not commute, so it *is* possible for this term to contribute to F_Q. However, it was shown in [15] that F_Q depends only on the variance of the angular momentum of the final state, and the use of attractive interactions to create solitons does not significantly effect the angular momentum in their system, indicating once again that this may be an artefact of the mean-field model.

However, we do not claim that there is no benefit at all to the use of solitons. It was observed in the experiment of McDonald *et al.* [16] that the maximum sensitivity was achieved when the scattering length was tuned to create a soliton. The reason for this was likely that the reduction in dispersion reduced various sources of technical noise in the experiment. Furthermore, the two soliton wave-packets remained overlapping for the duration of the experiment, so the system would not be subjected to the relative phase shearing noise reported in this manuscript. Additionally, the experiment was not operating at the SQL so it is unlikely that this noise source would be observed.

Finally, we note that it has been shown that soliton dynamics can create non-classical states [43–46]. However, it has yet to be shown that these states can be used for enhanced matterwave interferometry, as they will be subject to the same phase diffusion which is the subject of this manuscript.

Acknowledgements— The author would like to acknowledge useful discussions with Samuel Nolan, Matthew Davis, Joel Corney, Murray Olsen, Stuart Szigeti, Michael Bromley, John Helm, and Nick Robins. The numerical simulations were performed with XMDS2 [47] on the University of Queensland School of Mathematics and Physics computing cluster "Dogmatix", with thanks to Ian Mortimer for computing support. This work was supported by the European Union's Horizon 2020 research and innovation programme under the Marie Sklodowska-Curie grant agreement No. 704672.

* simon.a.haine@gmail.com

[1] A. D. Cronin, J. Schmiedmayer, and D. E. Pritchard, Rev. Mod. Phys. **81**, 1051 (2009).

[2] F. Riehle, T. Kisters, A. Witte, J. Helmcke, and C. J. Bordé, Phys. Rev. Lett. **67**, 177 (1991).

[3] T. L. Gustavson, P. Bouyer, and M. A. Kasevich, Phys. Rev. Lett. **78**, 2046 (1997).

[4] A. Lenef, T. D. Hammond, E. T. Smith, M. S. Chapman, R. A. Rubenstein, and D. E. Pritchard, Phys. Rev. Lett. **78**, 760 (1997).

[5] T. L. Gustavson, A. Landragin, and M. A. Kasevich, Classical and Quantum Gravity **17**, 2385 (2000).

[6] D. S. Durfee, Y. K. Shaham, and M. A. Kasevich, Phys. Rev. Lett. **97**, 240801 (2006).

[7] B. Canuel, F. Leduc, D. Holleville, A. Gauguet, J. Fils, A. Virdis, A. Clairon, N. Dimarcq, C. J. Bordé, A. Landragin, and P. Bouyer, Phys. Rev. Lett. **97**, 010402 (2006).

[8] S. M. Dickerson, J. M. Hogan, A. Sugarbaker, D. M. S. Johnson, and M. A. Kasevich, Phys. Rev. Lett. **111**, 083001 (2013).

[9] C. L. G. Alzar, W. Yan, and A. Landragin, in *Research in Optical Sciences* (Optical Society of America, 2012) p. JT2A.10.

[10] P. L. Halkyard, M. P. A. Jones, and S. A. Gardiner, Phys. Rev. A **81**, 061602 (2010).

[11] M. C. Kandes, R. Carretero-Gonzalez, and M. W. J. Bromley, arXiv:1306.1308 (2013).

[12] R. Stevenson, M. R. Hush, T. Bishop, I. Lesanovsky, and T. Fernholz, Phys. Rev. Lett. **115**, 163001 (2015).

[13] S. P. Nolan, J. Sabbatini, M. W. J. Bromley, M. J. Davis, and S. A. Haine, Phys. Rev. A **93**, 023616 (2016).

[14] T. A. Bell, J. A. P. Glidden, L. Humbert, M. W. J. Bromley, S. A. Haine, M. J. Davis, T. W. Neely, M. A. Baker, and H. Rubinsztein-Dunlop, New Journal of Physics **18**, 035003 (2016).

[15] S. A. Haine, Phys. Rev. Lett. **116**, 230404 (2016).

[16] G. D. McDonald, C. C. N. Kuhn, K. S. Hardman, S. Bennetts, P. J. Everitt, P. A. Altin, J. E. Debs, J. D. Close, and N. P. Robins, Phys. Rev. Lett. **113**, 013002 (2014).

[17] Y. V. Kartashov, B. A. Malomed, and L. Torner, Rev. Mod. Phys. **83**, 247 (2011).

[18] K. E. Strecker, G. B. Partridge, A. G. Truscott, and R. G. Hulet, Nature **417**, 150 (2002).

[19] L. Khaykovich, F. Schreck, G. Ferrari, T. Bourdel, J. Cubizolles, L. D. Carr, Y. Castin, and C. Salomon, Science **296**, 1290 (2002).

[20] K. E. Strecker, G. B. Partridge, A. G. Truscott, and R. G. Hulet, New Journal of Physics **5**, 73 (2003).

[21] S. L. Cornish, S. T. Thompson, and C. E. Wieman, Phys. Rev. Lett. **96**, 170401 (2006).

[22] A. L. Marchant, T. P. Billam, T. P. Wiles, M. M. H. Yu, S. A. Gardiner, and S. L. Cornish, Nature Communications **4**, 1865 EP (2013).

[23] J. Polo and V. Ahufinger, Phys. Rev. A **88**, 053628 (2013).

[24] J. Cuevas, P. G. Kevrekidis, B. A. Malomed, P. Dyke, and R. G. Hulet, New Journal of Physics **15**, 063006 (2013).

[25] J. L. Helm, S. L. Cornish, and S. A. Gardiner, Phys. Rev. Lett. **114**, 134101 (2015).

[26] A. Negretti and C. Henkel, Journal of Physics B: Atomic, Molecular and Optical Physics **37**, L385 (2004).

[27] N. Veretenov, Y. Rozhdestvensky, N. Rosanov, V. Smirnov, and S. Fedorov, The European Physical Journal D **42**, 455 (2007).

[28] S. J. Carter, P. D. Drummond, M. D. Reid, and R. M. Shelby, Phys. Rev. Lett. **58**, 1841 (1987).

[29] H. A. Bachor and T. C. Ralph, *A Guide to Experiments in Quantum Optics*, 2nd ed. (Wiley, 2004).

[30] P. A. Altin, G. McDonald, D. Döring, J. E. Debs, T. H. Barter, J. D. Close, N. P. Robins, S. A. Haine, T. M. Hanna, and R. P. Anderson, New Journal of Physics **13**, 065020 (2011).

[31] N. P. Robins, C. Figl, S. A. Haine, A. K. Morrison, M. Jeppesen, J. J. Hope, and J. D. Close, Phys. Rev. Lett. **96**, 140403 (2006).

[32] The only effect of g_{+-} is a slight modification of the velocity of the wavepackets, slightly altering the collision time T.

[33] S. A. Haine and M. T. Johnsson, Phys. Rev. A **80**, 023611 (2009).

[34] J. M. Radcliffe, Journal of Physics A: General Physics **4**, 313 (1971).

[35] P. D. Drummond and A. D. Hardman, EPL (Europhysics Letters) **21**, 279 (1993).

[36] M. J. Steel, M. K. Olsen, L. I. Plimak, P. D. Drummond, S. M. Tan, M. J. Collett, D. F. Walls, and R. Graham, Phys. Rev. A **58**, 4824 (1998).

[37] P. B. Blakie, A. S. Bradley, M. J. Davis, R. J. Ballagh, and C. W. Gardiner, *Advances in Physics*, Advances in Physics **57**, 363 (2008).

[38] M. T. Johnsson and S. A. Haine, Phys. Rev. Lett. **99**, 010401 (2007).

[39] S. A. Haine and A. J. Ferris, Phys. Rev. A **84**, 043624 (2011).

[40] S. A. Haine, J. Lau, R. P. Anderson, and M. T. Johnsson, Phys. Rev. A **90**, 023613 (2014).

[41] See Supplemental Material.

[42] R. Demkowicz-Dobrzański, M. Jarzyna, and J. Kołodyński, Progress in Optics **345** (2015).

[43] C. Weiss and Y. Castin, Phys. Rev. Lett. **102**, 010403 (2009).

[44] A. I. Streltsov, O. E. Alon, and L. S. Cederbaum, Phys. Rev. A **80**, 043616 (2009).

[45] M. Lewenstein and B. A. Malomed, New Journal of Physics **11**, 113014 (2009).

[46] B. Gertjerenken, T. P. Billam, C. L. Blackley, C. R. Le Sueur, L. Khaykovich, S. L. Cornish, and C. Weiss, Phys. Rev. Lett. **111**, 100406 (2013).

[47] G. R. Dennis, J. J. Hope, and M. T. Johnsson, Computer Physics Communications **184**, 201 (2013).

SUPPLEMENTAL MATERIAL: QUANTUM NOISE IN SOLITON MATTER-WAVE INTERFEROMETRY

In this supplemental material we provide further details on the calculations in the main text. Specifically, we derive the rotation angle required for the pre-twisting scheme.

Derivation of θ_χ

The angle required for our pre-twisting scheme, θ_χ, is the angle such that rotation about the J_x axis returns the variance of J_z to its original value, as illustrated in Fig. 4.

The action of the variable angle beamsplitter $\hat{U}_\theta = \exp(i\theta_\chi \hat{J}_x)$ on the psuedo-spin operators before ($t = T$) and after ($t = t_1$) the rotation is

$$\hat{J}_z(t_1) = \hat{U}_\theta^\dagger \hat{J}_z(T)\hat{U}_\theta = \hat{J}_z(T)\cos\theta_\chi + \hat{J}_y(T)\sin\theta_\chi \tag{9}$$

$$\hat{J}_y(t_1) = \hat{U}_\theta^\dagger \hat{J}_y(T)\hat{U}_\theta = \hat{J}_y(T)\cos\theta_\chi + \hat{J}_z(T)\sin\theta_\chi\,. \tag{10}$$

Therefore, after the rotation, the variance in $\hat{J}_z$ is

$$\begin{aligned} V(\hat{J}_z(t_1)) &= \langle \hat{J}_z^2(t_1)\rangle \\ &= \langle \hat{J}_z^2(T)\rangle \cos^2\theta_\chi + \langle \hat{J}_y^2(T)\rangle \sin^2\theta_\chi \\ &\quad + \cos\theta_\chi \sin\theta_\chi \left(\langle \hat{J}_z(T)\hat{J}_y(T)\rangle + \langle \hat{J}_y(T)\hat{J}_z(T)\rangle \right), \end{aligned} \tag{11}$$

since the state is chosen such that $\langle \hat{J}_z(t_1)\rangle = \langle \hat{J}_z(T)\rangle = 0$. The evolution under $\hat{U}_\chi = \exp(-i\mathcal{H}_{\rm int}T)$ commutes with $\hat{J}_z$, so $\langle \hat{J}_z^2(T)\rangle = \langle \hat{J}_z^2(0)\rangle = N_t/4$. The angle θ_χ is defined as the angle such that $\langle \hat{J}_z^2(t_1)\rangle = \langle \hat{J}_z^2(T)\rangle = N_t/4$. Expressing the pseudo-spin operators in terms of bosonic creation and annihilation operators, and making the substitution $\hat{a}_+ \to \hat{a}$ and $\hat{a}_- \to \hat{b}$ for ease of notation gives

$$\hat{J}_z^2 = \frac{1}{4}\left(\hat{a}^\dagger\hat{a}^\dagger\hat{a}\hat{a} + \hat{b}^\dagger\hat{b}^\dagger\hat{b}\hat{b} + \hat{a}^\dagger\hat{a} + \hat{b}^\dagger\hat{b} - 2\hat{a}^\dagger\hat{a}\hat{b}^\dagger\hat{b}\right) \tag{12}$$

$$\hat{J}_y^2 = \frac{1}{4}\left(2\hat{a}^\dagger\hat{a}\hat{b}^\dagger\hat{b} + \hat{a}^\dagger\hat{a} + \hat{b}^\dagger\hat{b} - \hat{a}^\dagger\hat{a}^\dagger\hat{b}\hat{b} - \hat{b}^\dagger\hat{b}^\dagger\hat{a}\hat{a}\right) \tag{13}$$

$$\hat{J}_z\hat{J}_y + \hat{J}_y\hat{J}_z = \frac{i}{2}\left(\hat{a}^\dagger\hat{a}\hat{a}\hat{b}^\dagger + \hat{a}^\dagger\hat{b}^\dagger\hat{b}\hat{b} - \hat{a}\hat{b}^\dagger\hat{b}^\dagger\hat{b} - \hat{a}^\dagger\hat{a}^\dagger\hat{a}\hat{b}\right) \tag{14}$$

In order to evaluate these expressions, we need to calculate terms such as $\langle \hat{a}^\dagger\hat{a}^\dagger\hat{a}\hat{b}\rangle$ with respect to the state

$$|\Psi(T)\rangle = e^{-2|\alpha|^2}\sum_{n_1=0}^{\infty}\sum_{n_2=0}^{\infty}\frac{\alpha^{n_1}}{\sqrt{n_1!}}\frac{\alpha^{n_2}}{\sqrt{n_2!}}|n_1,n_2\rangle e^{-i\Phi_{n_1,n_2}}\,, \tag{15}$$

where

$$\Phi_{n_1,n_2} = \frac{1}{2}\chi T\left[n_1(n_1-1) + n_2(n_2-1)\right], \tag{16}$$

and $\alpha = \sqrt{N_t/2}$. We will explicitly compute one example, and provide the rest of these operator moments in a table.

$$\begin{aligned}
\langle \hat{a}^\dagger \hat{a}^\dagger \hat{a} \hat{b} \rangle &= e^{-2|\alpha|^2} \sum_{m_1=0}^{\infty} \sum_{m_2=0}^{\infty} \sum_{n_1=0}^{\infty} \sum_{n_2=0}^{\infty} \frac{(\alpha^*)^{m_1} (\alpha^*)^{m_2} \alpha^{n_1} \alpha^{n_2}}{\sqrt{m_1! m_2! n_1! n_2!}} \langle m_1, m_2 | \hat{a}^\dagger \hat{a}^\dagger \hat{a} \hat{b} | n_1, n_2 \rangle e^{i(\Phi_{m_1,m_2} - \Phi_{n_1,n_2})} \\
&= e^{-2|\alpha|^2} \sum_{m_1=0}^{\infty} \sum_{m_2=0}^{\infty} \sum_{n_1=1}^{\infty} \sum_{n_2=1}^{\infty} \frac{(\alpha^*)^{m_1} (\alpha^*)^{m_2} \alpha^{n_1} \alpha^{n_2}}{\sqrt{m_1! m_2! n_1! n_2!}} n_1 \sqrt{n_1 + 1} \sqrt{n_2} \langle m_1, m_2 | n_1 + 1, n_2 - 1 \rangle e^{i(\Phi_{m_1,m_2} - \Phi_{n_1,n_2})} \\
&= e^{-2|\alpha|^2} \sum_{m_1=0}^{\infty} \sum_{m_2=0}^{\infty} \sum_{n_1=1}^{\infty} \sum_{n_2=1}^{\infty} \frac{(\alpha^*)^{m_1} (\alpha^*)^{m_2} \alpha^{n_1} \alpha^{n_2}}{\sqrt{m_1! m_2! n_1! n_2!}} n_1 \sqrt{n_1 + 1} \sqrt{n_2} e^{i(\Phi_{m_1,m_2} - \Phi_{n_1,n_2})} \delta_{m_1, n_1+1} \delta_{m_2, n_2 - 1} \\
&= e^{-2|\alpha|^2} \sum_{m_2=0}^{\infty} \sum_{n_1=1}^{\infty} \frac{(\alpha^*)^{n_1+1} (\alpha^*)^{m_2} \alpha^{n_1} \alpha^{m_2+1}}{\sqrt{(n_1+1)! m_2! n_1! (m_2+1)!}} n_1 \sqrt{n_1 + 1} \sqrt{m_2 + 1} e^{i\chi T (n_1 - m_2)} \\
&= |\alpha|^4 e^{i\chi T} e^{-2|\alpha|^2} \sum_{m_2=0}^{\infty} \sum_{n_1=1}^{\infty} \frac{(|\alpha|^2 e^{i\chi T})^{n_1 - 1}}{(n_1 - 1)!} \frac{(|\alpha|^2 e^{-i\chi T})^{m_2}}{m_2!} \\
&= |\alpha|^4 e^{i\chi T} e^{-2|\alpha|^2} e^{|\alpha|^2 e^{i\chi T}} e^{|\alpha|^2 e^{-i\chi T}} \\
&= \frac{N_t^2}{4} e^{i\chi T} \exp\left(N_t (\cos \chi T - 1) \right) . \qquad (17)
\end{aligned}$$

The complete set of moments required to calculate $\langle \hat{J}_z^2(t_1) \rangle$ is

$$\langle \hat{a}^\dagger \hat{a} \rangle = \langle \hat{b}^\dagger \hat{b} \rangle = \frac{N_t}{2} \qquad (18a)$$

$$\langle \hat{a}^\dagger \hat{a}^\dagger \hat{a} \hat{a} \rangle = \langle \hat{b}^\dagger \hat{b}^\dagger \hat{b} \hat{b} \rangle = \frac{N_t^2}{4} \qquad (18b)$$

$$\langle \hat{a}^\dagger \hat{a}^\dagger \hat{b} \hat{b} \rangle = \langle \hat{a} \hat{a} \hat{b}^\dagger \hat{b}^\dagger \rangle = \frac{N_t^2}{4} \exp\left[-N_t \sin^2(2\chi T) \right] \qquad (18c)$$

$$\langle \hat{a}^\dagger \hat{a}^\dagger \hat{a} \hat{b} \rangle = \langle \hat{a} \hat{b}^\dagger \hat{b}^\dagger \hat{b} \rangle = \frac{N_t^2}{4} e^{i\chi T} \exp\left[N_t (\cos \chi T - 1) \right] \qquad (18d)$$

$$\langle \hat{a}^\dagger \hat{a} \hat{a} \hat{b}^\dagger \rangle = \langle \hat{a}^\dagger \hat{b}^\dagger \hat{b} \hat{b} \rangle = \frac{N_t^2}{4} e^{-i\chi T} \exp\left[N_t (\cos \chi T - 1) \right] . \qquad (18e)$$

The solution to $\langle \hat{J}_z^2(t_1) \rangle = \langle \hat{J}_z^2(T) \rangle$ for θ_χ gives four non-trivial solutions:

$$\theta_\chi = \cos^{-1}(\gamma) \qquad (19a)$$

$$\theta_\chi = \cos^{-1}(-\gamma) \qquad (19b)$$

$$\theta_\chi = -\cos^{-1}(\gamma) \qquad (19c)$$

$$\theta_\chi = -\cos^{-1}(-\gamma) , \qquad (19d)$$

where

$$\begin{aligned}
\gamma &= \frac{\langle \hat{J}_z^2(T) \rangle - \langle \hat{J}_y^2(T) \rangle}{\sqrt{\langle \hat{J}_z^2(T) \rangle^2 + \langle \hat{J}_y^2(T) \rangle^2 + \langle \hat{J}_z(T) \hat{J}_y(T) + \hat{J}_y(T) \hat{J}_z(T) \rangle^2 - 2 \langle \hat{J}_z^2(T) \rangle \langle \hat{J}_y^2(T) \rangle}} \\
&= \frac{\left(\exp(2N_t \sin^2 \chi T) - 1 \right)}{\sqrt{\left(\exp(2N_t \sin^2 \chi T) - 1 \right)^2 + 16 \sin^2 \chi T \exp\left(2N_t (\cos \chi T - \cos 2\chi T) \right)}} . \qquad (20)
\end{aligned}$$

Of those solutions, the only one that gives better performance than the single loop scheme is Eq. (19d), which is what was used for both the two-mode and multi-mode pre-twisting calculations.

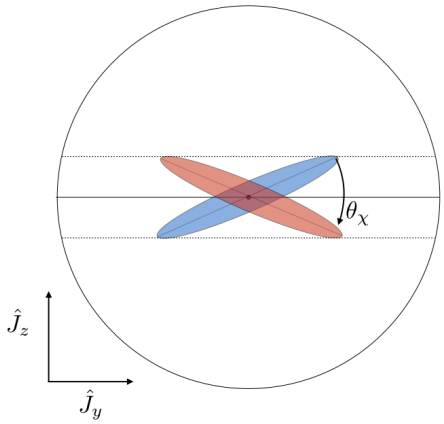

FIG. 4. (Color Online) The rotation angle θ_χ about the J_x axis required for re-phasing after a second application of $\hat{U}_\chi$ is the angle that has the same variance in $\hat{J}_z$ before and after rotation.